

# Faraday Discussions

Accepted Manuscript



This manuscript will be presented and discussed at a forthcoming Faraday Discussion meeting. All delegates can contribute to the discussion which will be included in the final volume.

**Register now to attend!** Full details of all upcoming meetings: <http://rsc.li/fd-upcoming-meetings>



This is an *Accepted Manuscript*, which has been through the Royal Society of Chemistry peer review process and has been accepted for publication.

*Accepted Manuscripts* are published online shortly after acceptance, before technical editing, formatting and proof reading. Using this free service, authors can make their results available to the community, in citable form, before we publish the edited article. We will replace this *Accepted Manuscript* with the edited and formatted *Advance Article* as soon as it is available.

You can find more information about *Accepted Manuscripts* in the [Information for Authors](#).

Please note that technical editing may introduce minor changes to the text and/or graphics, which may alter content. The journal's standard [Terms & Conditions](#) and the [Ethical guidelines](#) still apply. In no event shall the Royal Society of Chemistry be held responsible for any errors or omissions in this *Accepted Manuscript* or any consequences arising from the use of any information it contains.

## **Microtubule targeted therapeutics loaded polymeric assembled nanospheres for potentiation of antineoplastic activity**

Radhika Poojari,\* Rohit Srivastava and Dulal Panda\*

*Department of Biosciences and Bioengineering, Indian Institute of Technology Bombay, Mumbai 400076, India. E-mail: drradhipoojari@gmail.com; panda@iitb.ac.in; Tel: +91-22-25767838*

Polymeric nanoassemblies represent an attractive strategy for efficient cellular internalization of microtubule targeted anticancer drugs. Using the dynamic light scattering, zeta-potential, transmission electron microscopy and scanning electron microscopy, the physical properties and surface morphology of microtubule-binding PEGylated PLGA assembled nanospheres (100-200 nm) were analyzed. The present approach leads to strong internalization as observed by confocal laser scanning microscopy and transmission electron microscopy in hepatocarcinoma cells. The effect of these nanoassemblies on microtubules and mitosis were explored using immunofluorescence microscopy. The effects of these nanoassemblies on cancer cell proliferation and cell death revealed its antitumor enhancing effects. Perturbation of the microtubule assembly, mitosis and nuclear modulations potentiated the antineoplastic effects delivered via nanospheres in Hepatocarcinoma cells. The extensive biomolecular and physical characterizations of the synthesized nanoassemblies will help to design potent therapeutic materials and the present approach can be applied to deliver microtubule-targeted drugs for liver cancer therapy.

## 1. Introduction

Liver cancer is one of the most common causes of cancer-related mortality. Development of multidrug resistance, poor drug penetration into solid tumors, poor target selection and abnormal apoptosis machinery are found to decrease the efficacy of liver cancer chemotherapy.<sup>1-3</sup> Certain aberrantly expressed proteins in liver cancer lead to dysregulation in the proliferative and apoptotic signaling pathways, cell cycle anomalies and other pathways, which promote the growth of liver cancer cells.<sup>4,5</sup> Despite invasive chemotherapy, the survival rate of liver cancer patients is poor. Thus, nanotechnology based novel strategies can be helpful in designing new therapies against liver cancer. One such approach could be the use of nanoformulations to deliver microtubule-targeted drugs in solid tumors like liver cancer.

Microtubules (MT) are formed by the polymerization of a heterodimeric protein tubulin. MTs display a dynamic state of instability comprising of polymerization and depolymerization cycles.<sup>6-9</sup> The MT cytoskeleton is critical for cellular processes like mitosis, spindle formation, intracellular transport and locomotion. Killing cancer cells by disrupting the microtubules is one of the effective therapeutic strategies. Estradiol is a naturally occurring estrogen present in mammals, which is catalyzed from 2-hydroxyestradiol by catechol-Omethyltransferase (COMT) having no estrogen-related mitogenic activity.<sup>10-12</sup> Estradiol is a potent microtubule-targeted anticancer agent. It disrupts microtubule functioning, which then leads to cell cycle arrest at G2/M-phase.<sup>10-12</sup> It has also been reported to possess antiangiogenesis effect. Clinical drawbacks such as poor water solubility, poor pharmacokinetics, short half-life and adverse drug effects like systemic-neurotoxicity are responsible for the

limited therapeutic window, which contributes to poor drug efficacy.<sup>13-16</sup> Nano drug delivery system (NDDS) is considered to be one of the best effective modalities to circumvent the above problems.<sup>17,18</sup> NDDS has several advantages.<sup>17,18</sup> For example, NDDS protects the drug from inactivation and metabolism. The colloidal NDDS are stable and sustained release of the drug from the NDDS into the blood stream reduces the side effects. Further, they are biocompatible and can accumulate at the tumor site by enhanced permeability and retention mechanism.<sup>17,18</sup> Therefore, the polymeric nanoassemblies are of considerable present interest and represent one of the promising materials for cancer therapy as well as imaging.<sup>19,20</sup> Earlier study reported the preparation of 2-methoxyestradiol (2-ME) microspheres based poly (DL-lactide-co-glycolide) (PLGA) by emulsion solvent extraction method for breast cancer therapy. The 2-ME PLGA microspheres of a particle size of  $55.44 \pm 12.21 \mu\text{m}$  exhibited a controlled release over 46 days, and could efficiently inhibit the growth of MCF-7 cells.<sup>21</sup> Shen *et al.*,<sup>22</sup> reported 2-ME nanosuspension preparation by nanoprecipitation-high-frequency ultrasonication method with particle size of  $168.4 \pm 3.2 \text{ nm}$ . This 2-ME nanosuspension exhibited significant suppression of Lewis lung carcinoma indicating it as a possible delivery mode for the lung cancer therapy. Estradiol loaded PLGA nanoparticles have been shown to improve oral bioavailability of the drug without any inflammatory response.<sup>23, 24</sup>

In a quest to find an effective delivery modality with low toxicity, we synthesized a formulation of PEGylated PLGA assembled nanospheres-based Estradiol delivery for potentiating the antineoplastic effects in human Huh7 Hepatocarcinoma cells. We analyzed the particle size, zeta potential, encapsulation efficiency and release profile of the PEGylated PLGA assembled nanospheres encapsulated Estradiol in Huh7

Hepatocarcinoma cells. Further, the *in vitro* cellular uptake, cytotoxicity and cell death proficiency of Estradiol entrapped in the nanospheres were examined in Huh7 Hepatocarcinoma cells. PEGylated PLGA assembled nanospheres encapsulated Estradiol treatment strongly depolymerized microtubules in these cells. We address two key questions in this paper; how do the synthesized polymeric PEGylated PLGA assembled nanospheres entrapped microtubule binding drugs inhibit the proliferation of liver cancer cells and how do the polymeric PEGylated PLGA assembled nanospheres influence the antineoplastic activity.

## 2. Experimental

### 2.1 Materials

Poly(D,L-lactide-co-glycolide) (PLGA, MW 17,000) was a kind provision from Purac Biomaterials, Netherlands. NH<sub>2</sub>-PEG<sub>2000</sub>-COOH was obtained from Jenkem Technology USA Inc., USA. Polyvinyl alcohol (PVA) was obtained from SD Fine-Chem. Ltd., Mumbai. The drug Estradiol, dyes Rhodamine B (RB), Sulforhodamine B (SRB) reagent and Hoechst 33258 were purchased from Sigma-Aldrich, USA. Annexin V/PI apoptosis detection kit was procured from BD Pharmingen (San Diego, USA). All other reagents used in the experiments were of analytical reagent grade.

### 2.2 Synthesis procedure of polymeric PEGylated PLGA assembled nanospheres

PEGylated PLGA was synthesized using NH<sub>2</sub>-PEG<sub>2000</sub>-COOH by 1-ethyl-3-(3-dimethylaminopropyl)carbodiimide hydrochloride (EDC) – Sulfo-N-hydroxysuccinimide (Sulfo-NHS) conjugation chemistry as described previously.<sup>25,26</sup> Estradiol loaded

PEGylated PLGA assembled nanospheres were prepared by oil-in-water emulsion-solvent evaporation method. The organic phase comprised of PEGylated PLGA polymer (25 mg) and antimicrotubule agent Estradiol (1 mg) dissolved in dimethylformamide. This organic phase in turn was emulsified with the aqueous phase containing 2.5% PVA as the surfactant as well as stabilizer. This emulsion was sonicated for 2 min. The organic solvents used for emulsion preparation were removed through solvent-evaporation using Rotavapor. The polymeric nanospheres were centrifuged at 20,000 x g for 20 min. The free drug Estradiol in the supernatant was removed, pellets were washed with deionized water and re-centrifuged for 20 min. The washing steps were done three to four times for the removal of excess surfactant and drug. The pellets were resuspended in phosphate buffered saline and then lyophilized. Dye RB (50 µg/mL) loaded PEGylated PLGA assembled nanospheres and PEGylated PLGA assembled nanospheres were prepared similarly as above with the dye and in absence of a drug or a dye, respectively. Only PLGA nanoparticles were prepared in the absence of PEG. PLGA nanoparticles, PEGylated PLGA assembled nanospheres and PEGylated PLGA assembled nanospheres encapsulated Estradiol was subjected to physico-chemical characterization.

### **2.3 Dynamic light scattering (DLS) and Zeta potential measurements**

The hydrodynamic particle size of PLGA nanoparticles, PEGylated PLGA assembled nanospheres and PEGylated PLGA assembled nanospheres encapsulated Estradiol at 0.1 mg/mL dispersed in Milli Q water after brief sonication was measured by DLS using a 632 nm red laser (DLS 90Plus, Brookhaven Instruments Corporation, USA) at 25°C (scattering angle of 90°). The surface charge of PLGA nanoparticles,

PEGylated PLGA assembled nanospheres and PEGylated PLGA assembled nanospheres encapsulated Estradiol was measured using ZetaPlus Zeta-potential analyzer (Brookhaven Instruments Corporation, USA) in Milli Q water (pH 7.0) at room temperature. Physical stability of the PEGylated PLGA assembled nanospheres encapsulated Estradiol on storage at 4°C as a suspension in PBS (pH 7.4) was monitored for one week. Estradiol encapsulation efficiency in the PLGA nanoparticles and PEGylated PLGA assembled nanospheres was measured by using UV spectrophotometer (Perkin Elmer, Lambda 25) and calculated as follows; Estradiol drug encapsulation efficiency (%) = (amount of loaded Estradiol/amount of Estradiol added) x 100%. All the measurements were repeated three times and their mean was calculated.

#### **2.4 Transmission electron microscopy (TEM)**

The size and surface morphology of the PEGylated PLGA assembled nanospheres and PEGylated PLGA assembled nanospheres encapsulated Estradiol were investigated using TEM (JEOL, JEM-2100 F, Japan) operating at 120 kV. Nanosphere suspension (0.1 mg/mL) was drop-casted on carbon-coated copper grid, negatively stained with 1% phosphotungstic acid and then air dried.

For ultrastructural cellular internalization study by TEM analysis, human Huh7 Hepatocarcinoma cells were grown in Dulbecco's Modified Eagle Medium (DMEM) supplemented with 10% fetal bovine serum and 1% penicillin-streptomycin (HiMedia, Mumbai) at 37°C with 5% CO<sub>2</sub> atmosphere. Huh7 cells ( $> 1 \times 10^6$  cells/mL) were then incubated with PEGylated PLGA assembled nanospheres and PEGylated PLGA assembled nanospheres encapsulated Estradiol at 25 µg/mL for 24 hr in 25 mm tissue culture flasks (Nunc, USA). Briefly, the untreated control cells and treated

cells were centrifuged, fixed in 2.5% glutaraldehyde and washed with PBS, followed by fixation in 1% osmium tetroxide. The cells were then subjected to dehydration in graded series of alcohol, embedded using DER 332-732 embedding kit (EMS, USA) and polymerized for 48 hr. These resin blocks with cells were sectioned using an ultramicrotome (Leica Ultracut UCT, Germany) and ultrathin sections (70 nm) were placed on 300 mesh Formvar and carbon coated copper grids (EMS, USA). The grids were then processed with uranyl acetate and lead citrate solutions as previously described to visualize the cellular ultrastructures.<sup>27</sup> Micrographs of internalization of the PEGylated PLGA assembled nanospheres, PEGylated PLGA assembled nanospheres encapsulated Estradiol and untreated control cells was taken on a TEM (FEI TECNAI, 12 BioTwin, Netherlands) operating at 80 kV.

## **2.5 Scanning electron microscopy (SEM)**

The morphology of the nanoparticles was observed using a SEM (JSM-7600 F, Japan). Prior to SEM application, the dried PEGylated PLGA assembled nanospheres and PEGylated PLGA assembled nanospheres encapsulated Estradiol were placed on a stub and coated with gold using a sputter gold coater Auto Fine Coater (JEOL, Tokyo, Japan).

## **2.6 Drug release profiles**

The release of Estradiol from PLGA nanoparticles and PEGylated PLGA assembled nanospheres was analyzed by dialyzing (dialysis bags, molecular weight cut off 12 kDa, HiMedia, Mumbai) the samples against phosphate buffered saline (PBS, pH 7.4) at 37°C. An aliquot (1 mL) was taken from the release medium at predetermined intervals and was then replaced with an equivalent volume of fresh PBS to maintain

the constant conditions. The percentage of Estradiol content released as a function of time was quantified using a UV spectrophotometer.

## **2.7 Confocal laser scanning microscopy (CLSM) for analysis of cellular internalization and MT interactions**

For intracellular uptake study by CLSM analysis, Huh7 cells ( $5 \times 10^4$  cells/well) were seeded on 12 mm glass cover-slips in 24 well plates (Nunc, USA). On reaching 70% confluency, the culture medium was replaced with PEGylated PLGA assembled nanospheres and PEGylated PLGA assembled nanospheres encapsulated RB at 50  $\mu\text{g/mL}$  for 24 hr of incubation, and then subjected to indirect immunocytochemistry CLSM analysis. Untreated cells were considered as the negative control. Images were acquired using CLSM (LSM 510 Meta, Carl Zeiss, Germany) equipped with a 63 $\times$  oil immersion objective lens and Zeiss LSM Image Browser software.

For evaluating the effect of PEGylated PLGA assembled nanospheres on microtubules by immunocytochemistry analysis, Huh7 cells ( $5 \times 10^4$  cells/well) in 24 well plates were subjected to treatment with 5.6  $\mu\text{M}$   $\text{IC}_{50}$  concentration of Estradiol and PEGylated PLGA assembled nanospheres encapsulated Estradiol for 48 hr. Untreated cells and PEGylated PLGA assembled nanospheres treated cells (50  $\mu\text{g/mL}$ ) were the negative controls. Cells were then fixed in 3.7% formaldehyde at 37°C for 30 min and subjected to immunostaining with primary antibody anti- $\alpha$ -Tubulin mouse monoclonal antibody (Sigma Aldrich, USA) which was followed by incubation with secondary antibody anti-mouse IgG-Alexa 568 conjugate (Invitrogen, USA). Hoechst 33258 was used for the nuclear staining and the cells were observed under CLSM.<sup>28,29</sup>

## **2.8 Antiproliferative analysis**

Cell viability was measured by SRB assay.<sup>30,31</sup> Hepatocarcinoma Huh7 cells were incubated in 96-well plates (Nunc, USA) at  $5 \times 10^4$  cells/well density and then subjected to treatment with PEGylated PLGA assembled nanospheres (50-250  $\mu\text{g/mL}$ ), free drug Estradiol (1-7  $\mu\text{M}$ ) and PEGylated PLGA assembled nanospheres encapsulated Estradiol (1-7  $\mu\text{M}$ ) for 48 hr to evaluate their antiproliferative activity. The absorbance was measured with a 96-well fluorescence plate reader (SPECTRAmax M2, Molecular Devices, USA) equipped with the SOFTmax Pro software (Molecular Devices), at a wavelength of 550 nm. The half maximal inhibitory concentration ( $\text{IC}_{50}$ ) values of free drug Estradiol vs PEGylated PLGA assembled nanospheres encapsulated Estradiol was analyzed by OriginPro 8.0 software.

## 2.9 Cell death analysis

The apoptosis activity in Huh7 cells was measured by Annexin V and Propidium iodide (PI) staining detection kit.<sup>28</sup> Huh7 cells ( $1 \times 10^5$  cells/mL) was seeded in 6-well plates and treated with Estradiol and PEGylated PLGA assembled nanospheres encapsulated Estradiol at the  $\text{IC}_{50}$  concentration (5.6  $\mu\text{M}$ ) for 48 hr. Untreated cells and PEGylated PLGA assembled nanospheres (50  $\mu\text{g/mL}$ ) treated cells were considered as the negative controls. Cells were washed twice with PBS and resuspended in  $1 \times$  binding buffer (400  $\mu\text{L}$ ). Later, Annexin V-FITC (5  $\mu\text{L}$ ) and PI solution (5  $\mu\text{L}$ ) were added to test samples, incubated in dark for 15 min at room temperature, and subsequently analyzed using a flow cytometer (BD FACS ARIA special order system equipped with BD FACSDiva, Becton and Dickinson, USA

software program). For each test sample, the fluorescence of ~ 20,000 cells was counted. Data represent the mean of three independent experiments.

### **2.10 Statistical evaluation**

The data represent mean  $\pm$  SD. Statistical evaluation was carried out using OriginPro 8.0 software.

## **3. Results and discussion**

### **3.1 PEGylated PLGA assembled nanospheres characterization – Size, shape, charge and stability matters**

PEGylated PLGA based drug delivery system has a number of advantages over other polymers used in drug, gene delivery and various biomedical applications, including biodegradability, biocompatibility, non-antigenicity, easy scale-up for manufacturing, and is a FDA approved polymer for human use.<sup>26,32</sup> It can be used for site-specific targeting and controlled-release of encapsulated drug. Also, PEG provides stealth surface effects, increases the stability and half-plasma life of the PEGylated PLGA nanoassemblies in order to prevent the non-specific interactions minimizing the side effects, decreases the phagocytic uptake, improves the bioavailability of the drug, and accumulates in tumour tissues.<sup>25,26,33</sup> Herein, we report the preparation of PEGylated PLGA assembled nanospheres encapsulated with microtubule-binding agent, Estradiol by an emulsion-solvent evaporation method using PVA as the emulsifier (Fig. 1). PEGylation of these polymeric nanospheres facilitated steric stability to the delivery system.

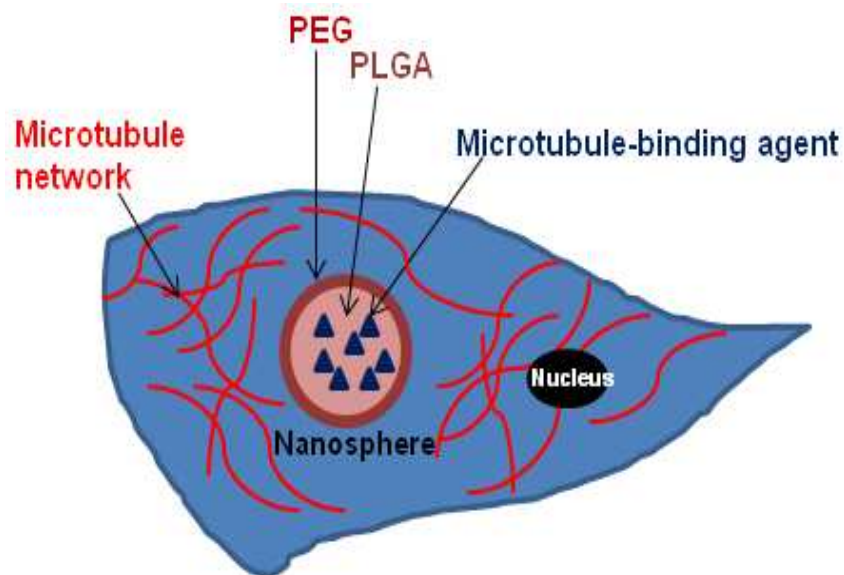


**Fig. 1** An illustration depicting a microtubule-binding chemotherapeutic agent encapsulated inside a polymeric PEGylated PLGA assembled nanosphere to target liver cancer cells.

The size and shape of the nanoparticles are known to greatly influence cellular internalization.<sup>32,34,35</sup> Spherical shaped nanoparticles have been reported to possess five times more uptake capacity than the rod shaped ones suggesting that the elongated nanoparticles required more time for the cellular endocytosis process.<sup>34</sup> The charge of the nanoparticles also influences their interaction with the cell membrane and thereby, affects the cellular internalization. Surface charge on particles can be explored to carry the cargo inside the cell.<sup>32,35</sup> DLS results of PLGA nanoparticles, PEGylated PLGA assembled nanospheres and PEGylated PLGA assembled nanospheres encapsulated Estradiol depicted a mean hydrodynamic diameter of  $211 \pm 8$ ,  $180 \pm 6$  and  $200 \pm 6$  nm and the zeta potential of  $-18.7 \pm 5.3$ ,  $-7.4 \pm 1.1$  and  $4.5 \pm 2.1$  mV, respectively. The mean polydispersity index

(PDI) of PLGA nanoparticles, PEGylated PLGA assembled nanospheres and PEGylated PLGA assembled nanospheres encapsulated Estradiol were  $0.27 \pm 0.06$ ,  $0.20 \pm 0.01$  and  $0.13 \pm 0.01$ , respectively. PDI of 0.13 indicated a narrow size distribution of the Estradiol loaded polymeric nanospheres, and well dispersion. The encapsulation efficiency was found to be  $36 \pm 5.1\%$  for PLGA nanoparticles and  $40 \pm 3.4\%$  for PEGylated PLGA assembled nanospheres by using the UV absorption spectroscopy. The physical stability of the PEGylated PLGA assembled nanospheres encapsulated Estradiol stored at  $4^{\circ}\text{C}$  was monitored for 1 week. No significant change either in the hydrodynamic size ( $209 \pm 4$  nm) or in the zeta potential ( $5.2 \pm 1.1$  mV) was observed in the samples after 1 week indicating the stealth effects of PEG.<sup>26,33</sup> TEM and SEM analysis of the synthesized PEGylated PLGA assembled nanospheres and PEGylated PLGA assembled nanospheres encapsulated Estradiol indicated nanospheres were spherical in shape with a smooth surface (Fig. 2A-E).

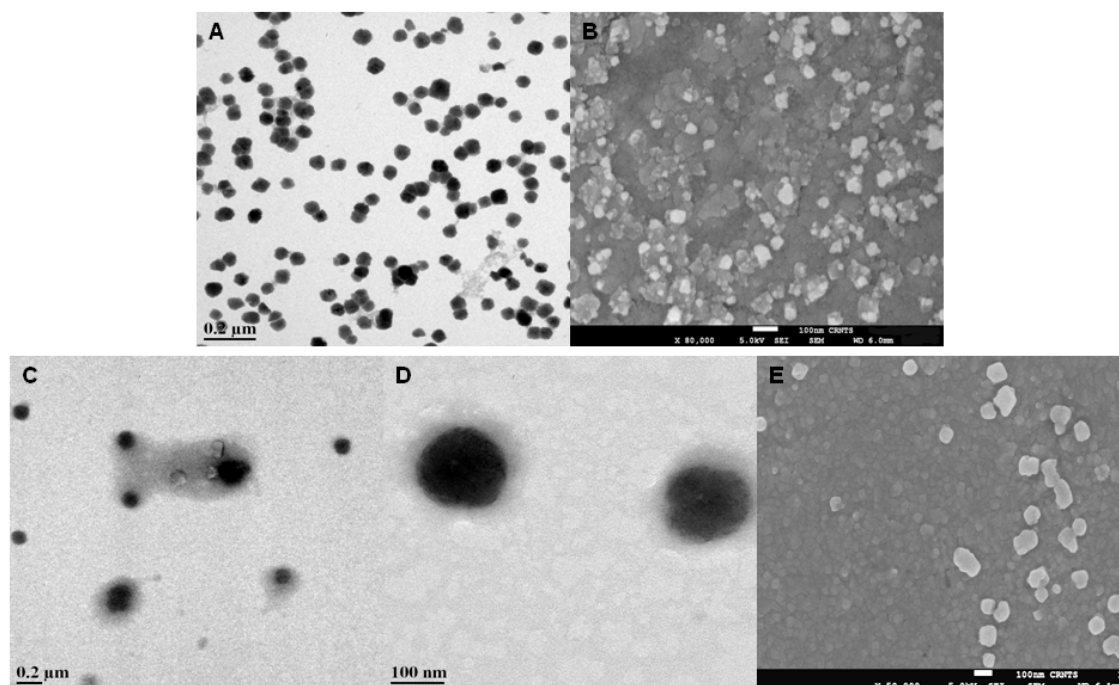


**Fig. 2.** (A) TEM and (B) SEM images of PEGylated PLGA assembled nanospheres. (C,D) TEM images at 200 nm and 100 nm scales, and (E) SEM image of PEGylated PLGA assembled nanospheres encapsulated Estradiol.

### 3.2 Estradiol release profiles

The cumulative Estradiol release from PLGA nanoparticles and PEGylated PLGA assembled nanospheres in PBS (pH 7.4) at 37°C has been shown in Fig. 3. PLGA nanoparticles showed a biphasic release pattern, which was characterized with an initial burst release of Estradiol followed by a sustained release. At 24 h, the amount of Estradiol released from PLGA nanoparticles in the initial burst was 51% and ~67% of drug was released at 72 h. No significant burst release of Estradiol was observed in the initial stages in case of PEGylated PLGA assembled nanospheres showing about 30% release in 24 h and about 42% release in 72 h, indicating its slow diffusion than the PLGA nanoparticles. The cumulative drug release in 10 days was

found to be 54% in PEGylated PLGA assembled nanospheres whereas it was 78% for PLGA nanoparticles, indicating that the sustained slower release of Estradiol was due to the presence of PEG, a stealth surface layer surrounding PLGA (i.e. PLGA core–PEG shell) nanospheres. Pegylation is known to impart increased circulation of drug delivery carriers for controlled and optimal drug release.<sup>36-38</sup> This inferred that PEGylated PLGA assembled nanospheres are suitable for prolonged Estradiol delivery system, which is in concurrence with the previous reports.<sup>36-38</sup>

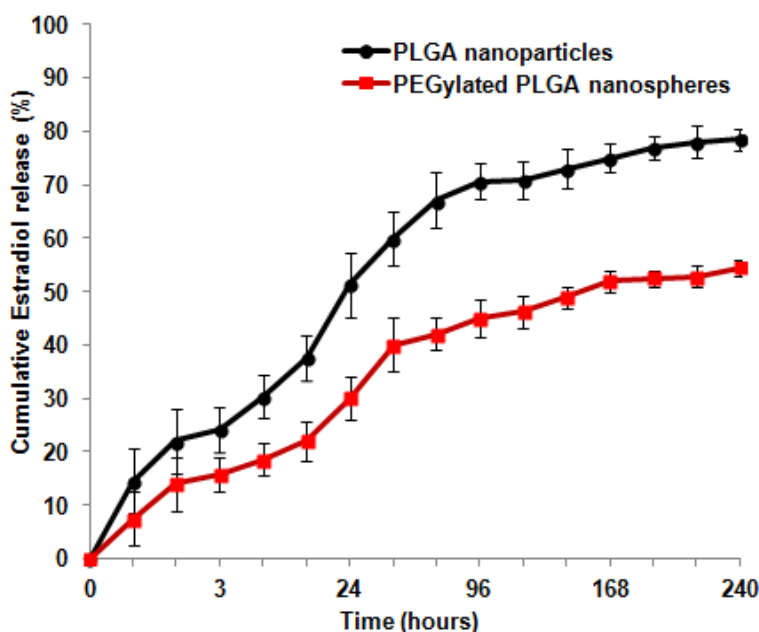


**Fig. 3.** The release profiles of Estradiol from PLGA nanoparticles and PEGylated PLGA assembled nanospheres in PBS at pH 7.4.

### 3.3 Influence of internalization of PEGylated PLGA assembled nanospheres

The delivery efficiency of our synthesized PEGylated PLGA assembled nanospheres was evaluated by the CLSM qualitative analysis of fluorescent dye RB taken up by the Huh7 cells. Cellular internalization is an important factor for the evaluation of

different drug delivery therapeutic modalities in cancer.<sup>17</sup> CLSM studies showed PEGylated PLGA assembled nanospheres RB (50  $\mu\text{g}/\text{mL}$ ) were readily internalized by Huh7 cells distributed in the cytoplasm (intense bright red fluorescence) in 24 hr (Fig. 4C). Untreated control cells and treatment with PEGylated PLGA assembled nanospheres (50  $\mu\text{g}/\text{mL}$ ) showed no fluorescence signal (Fig. 4A,B).

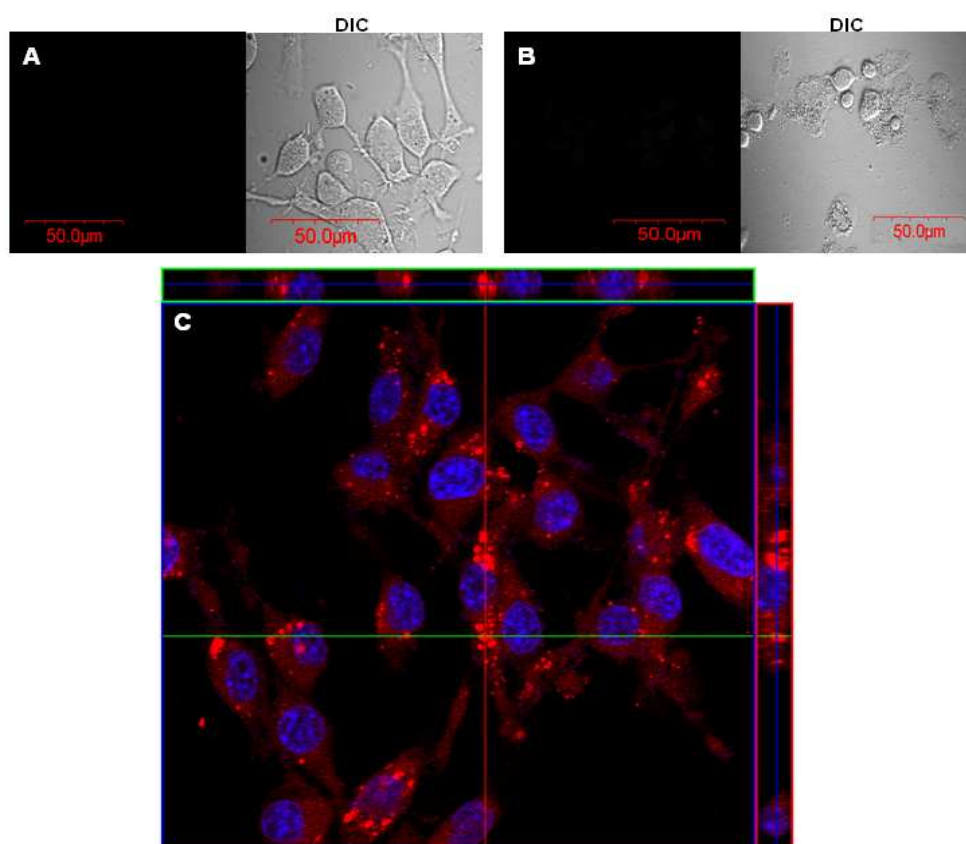


**Fig. 4.** Differential interference contrast (DIC) microscopy images of (A) Control cells, (B) PEGylated PLGA assembled nanospheres treated cells, and (C) CLSM reconstructions of Huh7 cells showing the intracellular distribution of PEGylated PLGA assembled nanospheres encapsulated RB at 24 hr. The PEGylated PLGA assembled nanospheres encapsulated RBs were seen as intense bright red fluorescence in the cells. Cell nuclei were stained with Hoechst 33258 (blue

fluorescence) and microtubule organization (anti- $\alpha$ -tubulin) are seen as light red fluorescence.

The ultrastructural studies of untreated control cells showed normal cellular architecture (Fig. 5A). PEGylated PLGA nanospheres (25  $\mu\text{g}/\text{mL}$ ) treated Huh7 cells by TEM revealed the intact structure of cell membrane and nucleus (Fig. 5B) whereas, disrupted cell membrane integrity, condensation of nucleus and nuclear fragmentation were clearly observed in the treated PEGylated PLGA assembled nanospheres encapsulated Estradiol (25  $\mu\text{g}/\text{mL}$ ) in 24 hr (Fig. 5C). It has been reported that the pegylation promotes cellular uptake due to an increase in the circulation time of nanoparticles.<sup>26,36,38</sup> Hence, from our results it can be inferred that PEGylated PLGA assembled nanospheres enhanced the RB cellular uptake and also enhanced the PEGylated PLGA assembled nanospheres encapsulated Estradiol internalization in Huh7 cells, which is in concurrence with the previous reports.<sup>26,36,38</sup>

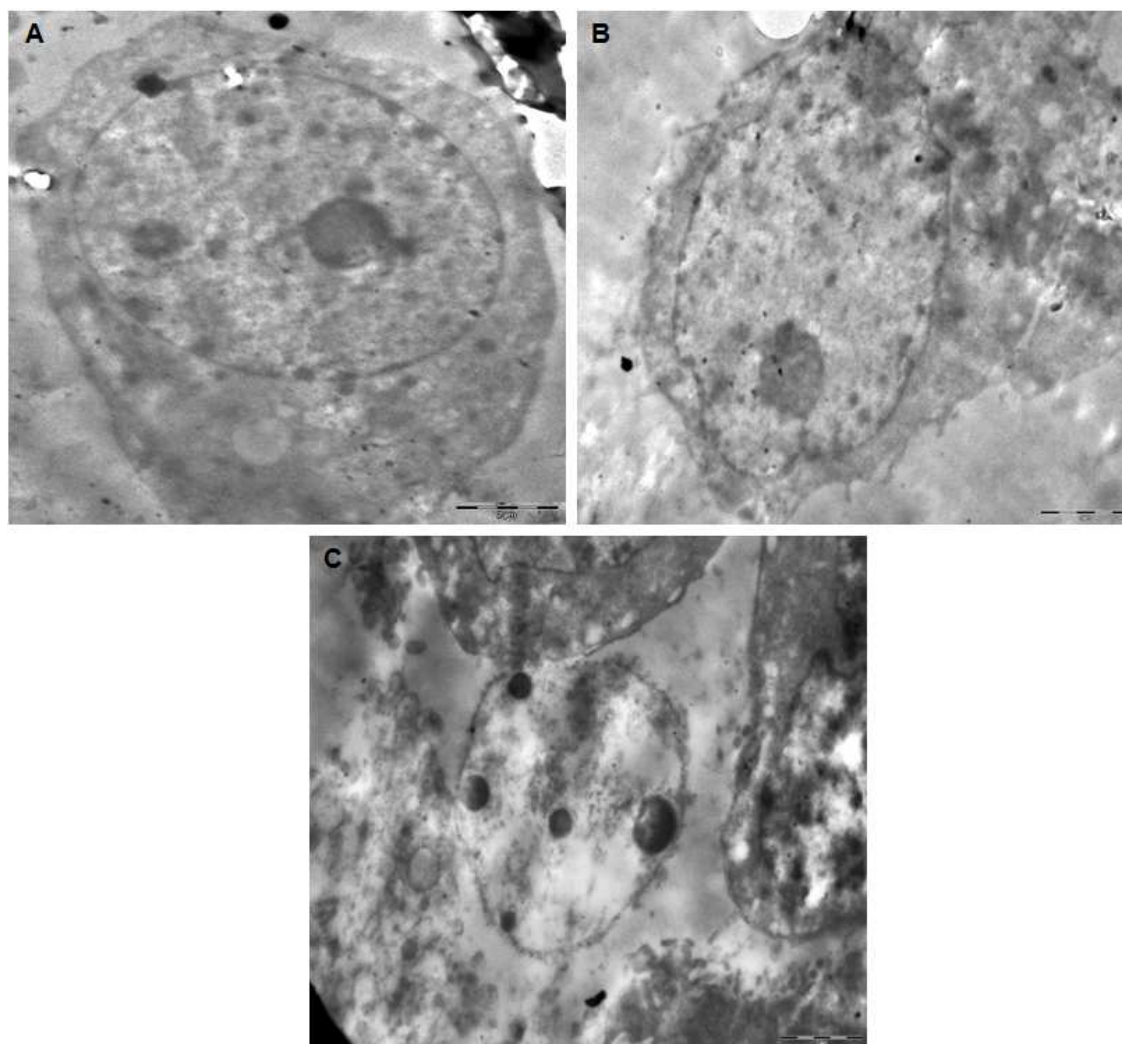


**Fig. 5.** Ultrastructural TEM images of Huh7 cells (A) Control cells, (B) treated with PEGylated PLGA assembled nanospheres and (C) treated with PEGylated PLGA assembled nanospheres encapsulated Estradiol showing efficient cellular internalization at 24 hr. Scale: 2  $\mu\text{m}$ .

### 3.4 Influence of PEGylated PLGA assembled nanospheres on cell proliferation

2-ME have been reported to induce cytotoxicity in prostate cancer cells.<sup>39</sup> Herein, the dose responses of PEGylated PLGA assembled nanospheres (50-250  $\mu\text{g/mL}$ ), free Estradiol (1-7  $\mu\text{M}$ ) and PEGylated PLGA assembled nanospheres encapsulated

Estradiol (1-7  $\mu\text{M}$ ) in Huh7 cells were evaluated by quantification of the total metabolic activity after 48 hr of exposure by SRB assay.<sup>30,31</sup> The delivery of PEGylated PLGA assembled nanospheres encapsulated Estradiol increased the cell killing efficiency in Huh7 cells. Antiproliferative effects of free Estradiol exhibited  $\text{IC}_{50}$  of  $5.6 \pm 0.8 \mu\text{M}$  in comparison to PEGylated PLGA assembled nanospheres encapsulated Estradiol with  $\text{IC}_{50}$  of  $2.2 \pm 0.5 \mu\text{M}$ . These results indicated enhanced cell growth inhibition via PEGylated PLGA assembled nanospheres encapsulated Estradiol in comparison to the free Estradiol. The drug loaded polymeric nanospheres were able to better internalize into the cells and efficiently deliver Estradiol in comparison to the free drug in the cells. PEGylated PLGA assembled nanospheres at 50, 100, 250 and 500  $\mu\text{g/mL}$  were non-toxic to cells with no significant difference in cell viabilities in comparison to the control cells, indicating its biocompatibility. Overall, the data suggested that PEGylated PLGA assembled nanospheres provided an efficient delivery modality for Estradiol.

### 3.5 Influence of PEGylated PLGA assembled nanospheres on cell death

A strategy that helps to accelerate tumor cell death remains a crucial factor in cancer chemotherapy.<sup>40,41</sup> Previous study have shown 2-ME to inhibit growth and induce apoptosis in prostate cancer cells by arresting the cells in G2/M phase.<sup>39</sup> Herein, the influence of PEGylated PLGA assembled nanospheres treatment on cell death were evaluated in Huh7 cells using Annexin V/PI assay at  $\text{IC}_{50}$  concentrations for 48 hr by flow cytometry as shown in Table 1 and Fig. 6. Cancer cells die through both apoptosis and necrosis. The data revealed that PEGylated PLGA assembled nanospheres encapsulated Estradiol induced greater cell death (apoptosis and necrosis) compared to that of the free drug at 5.6  $\mu\text{M}$ . ~6.5% of early apoptosis (i.e.

Annexin V stained positive cells) and ~3% of late apoptosis (i.e. PI stained cells of cells) were observed after treatment with Estradiol for 48 h in comparison to ~12% of early apoptosis and ~30% of late apoptosis of apoptosis were observed for PEGylated PLGA assembled nanospheres encapsulated Estradiol in Huh7 cells. No difference in the apoptotic rates were observed between the treated PEGylated PLGA assembled nanospheres and the control cells, indicating that the polymeric nanospheres by themselves did not elicit significant apoptosis. Increased circulation time of nanoparticles by pegylation has been reported in enhanced cell uptake, and thereby its therapeutic effects.<sup>26,36,38</sup> Hence, from the results it can be inferred that PEGylated PLGA assembled nanospheres encapsulated Estradiol could enhance the apoptosis induction effectively due to the efficient internalization by these polymeric nanospheres in comparison to the free Estradiol (Table 1 and Fig. 6).

**Table 1.** Cell death evaluation of PEGylated PLGA assembled nanospheres in Huh7 cells.

<b>Population (%)</b>	<b>Control</b>	<b>PEGylated PLGA assembled nanospheres</b>	<b>Estradiol</b>	<b>PEGylated PLGA assembled nanospheres encapsulated Estradiol</b>
<b>Live cells</b>	99.8	99.7	80.5	49.5
<b>Necrotic cells</b>	0.1	0.1	10	8.5
<b>Early apoptotic cells</b>	0.1	0.2	6.5	12
<b>Late apoptotic cells</b>	0	0	3	30

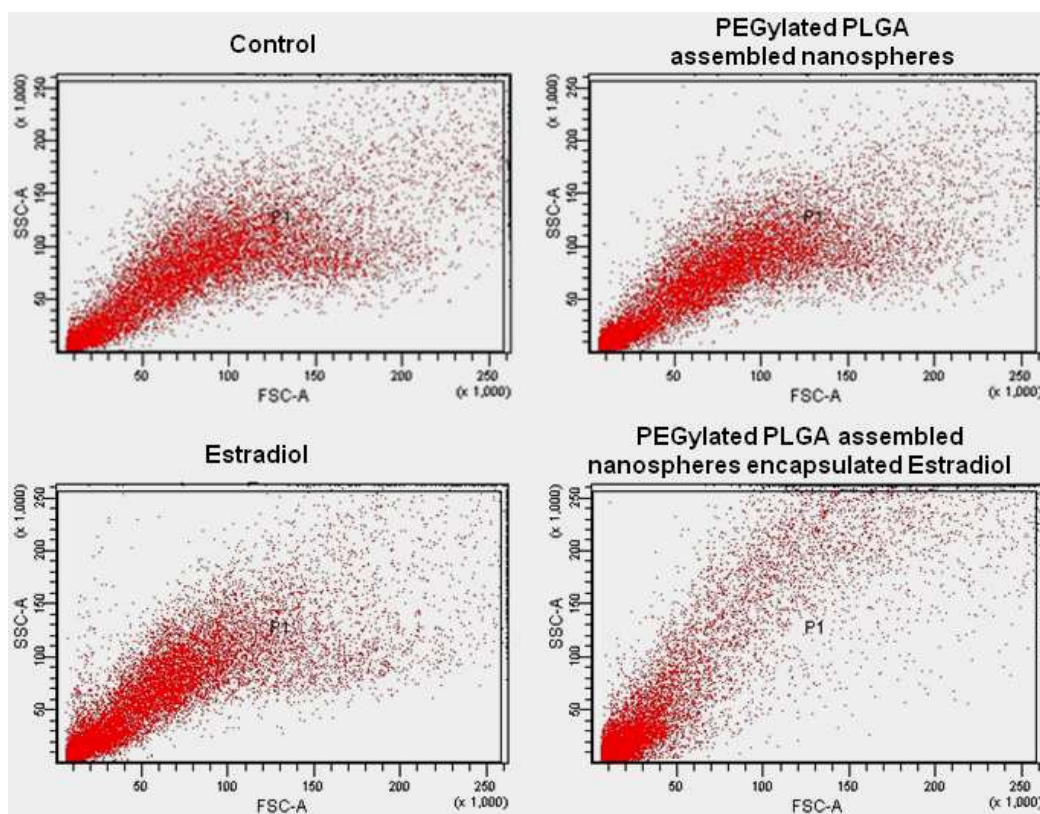


**Fig. 6.** PEGylated PLGA assembled nanospheres induced apoptosis in Huh7 cells. Cells were treated with PEGylated PLGA assembled nanospheres for 48 hr and analyzed by flow-cytometry.

### 3.6 Effects of PEGylated PLGA assembled nanospheres on microtubule organization in Huh7 cells

Estradiol binds at the colchicine site of  $\alpha$ -tubulin, interferes with the interphase and mitotic microtubules and causes mitotic arrest.<sup>10,12,42</sup> Immunocytochemistry revealed strong microtubule depolymerization, irregular cells and induction of multinucleation with PEGylated PLGA assembled nanospheres encapsulated Estradiol (Fig. 7D) in comparison to the free drug (Fig. 7C) in Huh7 cells. Estradiol was able to elicit less

activity wherein, microtubule cytoskeleton was not strongly disrupted. Morphological evidence of PEGylated PLGA assembled nanospheres encapsulated Estradiol treated cells with respect to nuclear alterations in the form of fragmented nuclei and apoptotic bodies were visible in Hoechst 33258 stained cells. A strong induction of multinucleation of cells indicated a well-disrupted mitotic division. Interestingly, morphologic alteration in the nuclei of Estradiol treated cells was not much effective. In case of PEGylated PLGA assembled nanospheres treated cells the microtubule cytoskeletal architecture was intact with no cell damage and the nuclear morphology was normal (Fig. 7A,B). The superior antineoplastic effect of PEGylated PLGA assembled nanospheres mediated Estradiol delivery in Huh7 cells in comparison to the free Estradiol reflects the efficient internalization via polymeric nanospheres leading to potent disruption of mitotic spindle apparatus and apparently cell death induction.

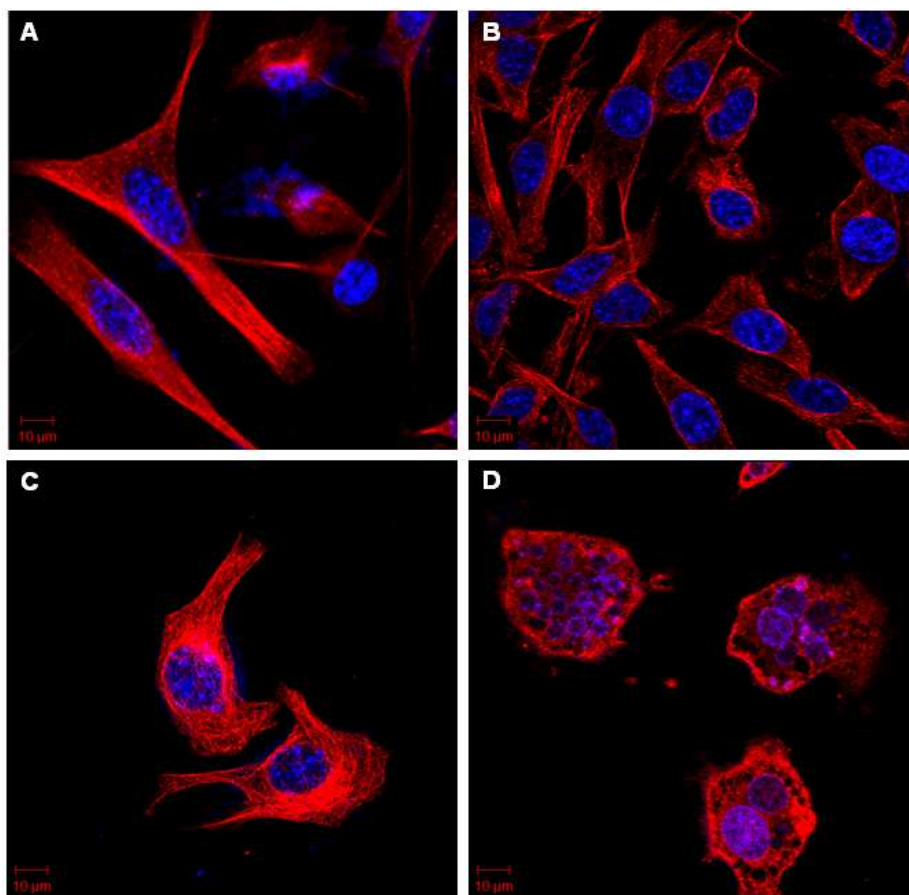


**Fig. 7.** Effects of the PEGylated PLGA assembled nanospheres and free drug on the microtubule organizations and nuclear morphology in Huh7 cells. (A) Control cells, (B) PEGylated PLGA assembled nanospheres (C) free drug Estradiol and (D) PEGylated PLGA assembled nanospheres encapsulated Estradiol treated cells for 48 hr at 5.6  $\mu\text{M}$ . Fixed cells were stained with anti- $\alpha$ -tubulin (red fluorescence) and the nucleus with Hoechst 33258 (blue fluorescence). Scale: 10  $\mu\text{m}$ .

#### 4. Conclusions

We report a strategy to effectively deliver Estradiol using PEGylated PLGA assembled nanospheres. The PEGylated PLGA assembled nanospheres encapsulated Estradiol strongly depolymerized microtubules, inhibited cell

proliferation and induced cell death in Huh7 Hepatocarcinoma cells in comparison to the free drug. Fluorescence and ultrastructural analysis suggested that PEGylated PLGA assembled nanospheres enhanced the internalization process of RB or Estradiol, respectively in Huh7 Hepatocarcinoma cells. PEGylated PLGA assembled nanospheres encapsulated Estradiol was found to be stable and potentiated the antineoplastic effects of the drug in Hepatocarcinoma cells. Further, scale-up of PEGylated PLGA assembled nanospheres encapsulated Estradiol and its evaluation in xenografted Hepatocarcinoma animal models need to be explored for translational research. The results discussed here provide insights into the development of microtubule-binding polymeric nanoassemblies for the treatment of hepatic neoplastic disorders.

### **Acknowledgements**

R. Poojari thanks DBT-Post doctoral fellowship in Biotechnology and Life Sciences, Government of India. The study was supported by DAE-SRC fellowship, Government of India to D. Panda. Authors thank Centre for Research in Nanotechnology and Science (CRNTS) for providing the characterization facility, S. Kini for help with the cell culture studies at IIT Bombay, India, and Advanced Centre for Treatment, Research and Education in Cancer (ACTREC), India for providing CLSM digital imaging facility.

### **Notes and references**

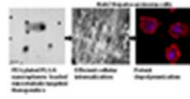
1. R. Siegel, J. Ma, Z. Zou and A. Jemal, *CA. Cancer J. Clin.*, 2014, **64**, 9–29.
2. H. El-Serag, *New Engl. J. Med.*, 2011, **365**, 1118–1127.

3. J. M. Llovet, A. Burroughs and J. Bruix, *Lancet*, 2003, **362**, 1907–1917.
4. X. Bisteau, M. J. Caldez and P. Kaldis, *Cancers (Basel)*, 2014, **6**, 79–111.
5. J. M. Llovet and J. Bruix, *Hepatology*, 2008, **48**, 1312–1327.
6. D. J. Needleman, M. A. Ojeda-Lopez, U. Raviv, H. P. Miller, Y. Li, C. Song, S. C. Feinstein, L. Wilson, M. C. Choi and C. R. Safinya, *Faraday Discuss.*, 2013, **166**, 31–45.
7. R. A. Stanton, K. M. Gernert, J. H. Nettles and R. Aneja, *Med. Res. Rev.*, 2011, **31**, 443–481.
8. M. A. Jordan and L. Wilson, *Nat. Rev. Cancer*, 2004, **4**, 253–265.
9. R. Mohan and D. Panda, *Cancer Res.*, 2008, **68**, 6181–6189.
10. Aizu-Yokota, K. Ichinoseki and Y. Sato, *Carcinogenesis*, 1994, **15**, 1875–1879.
11. J. Saussède-Aim, E.L. Matera, C. Ferlini and C. Dumontet, *Cell Motil. Cytoskeleton*, 2009, **66**, 378–388.
12. R.J. D'Amato and M. J. Folkman, *US Pat.*, 7,381,848 B2, 2008.
13. K. Pal, S. Pore, S. Sinha, R. Janardhanan, D. Mukhopadhyay and R. Banerjee, *J. Med. Chem.*, 2011, **54**, 2378–2390.
14. A. Gupta, P. Saha, C. Descôteaux, V. Leblanc, É. Asselin and G. Bérubé, *Bioorg. Med. Chem. Lett.*, 2010, **20**, 1614–1618.

15. M. R. Harrison, N. M. Hahn, R. Pili, W. K. Oh, H. Hammers, C. Sweeney, K. Kim, S. Perlman, J. Arnott, C. Sidor, G. Wilding and G. Liu, *Invest. New Drugs*, 2011, **29**, 1465–1474.
16. S. Verenich and P. M. Gerk, *Mol. Pharm.*, 2010, **7**, 2030–2039.
17. N. Kamaly, Z. Xiao, P. M. Valencia, A. F. Radovic-Moreno and O. C. Farokhzad, *Chem. Soc. Rev.*, 2012, **41**, 2971–3010.
18. M. Ferrari, *Nat. Rev. Cancer*, 2005, **5**, 161–171.
19. Z. Liu, Y. Wang and N. Zhang, *Expert Opin. Drug Deliv.*, 2012, **9**, 805–822.
20. H.J. Lee, A. Ponta and Y. Bae, *Ther. Deliv.* 2010,**1**, 803–817.
21. X. Guo, Q. Mei, Y. Xing, L. Ye, H. Zhang, X. Shi and Z. Zhang, *Drug Deliv.* 2012, **19**,143–148.
22. G. Shen, Q. Wang, Q. Zhang, H. Sun, Y. Zhao, Z. Zhang and B. Du, *Drug Deliv.* 2012, **19**, 327–333.
23. G. Mittal, D.K. Sahana, V. Bhardwaj and M.N.V. Ravi Kumar, *J. Control. Release*, 2007, **119**, 77–85.
24. D.K. Sahana, G. Mittal, V. Bhardwaj and M.N.V. Ravi Kumar, *J. Pharm. Sci.*, 2008, **97**, 1530–1542.
25. J. Cheng, B. A. Teply, I. Sherifi, J. Sung, G. Luther, F. X. Gu, E. Levy-Nissenbaum, A. F. Radovic-Moreno, R. Langer and O. C. Farokhzad, *Biomaterials*, 2007, **28**, 869–876.
26. F. Gu, L. Zhang, B. A. Teply, N. Mann, A. Wang, A. F. Radovic-Moreno, R. Langer, and O. C. Farokhzad, *Proc. Natl. Acad. Sci. USA*, 2008, **105**, 2586–2591.

27. A. M. Schrand, J. J. Schlager, L. Dai and S. M. Hussain, *Nat. Protoc.*, 2010, **5**, 744–757.
28. P. K. Gajula, J. Asthana, D. Panda and T. K. Chakraborty, *J. Med. Chem.*, 2013, **56**, 2235–2245.
29. A. Rai, T. K. Gupta, S. Kini, A. Kunwar, A. Surolia and D. Panda, *Biochem. Pharmacol.*, 2013, **86**, 378–391.
30. V. Vichai and K. Kirtikara, *Nat. Protoc.*, 2006, **1**, 1112–1116.
31. P. Skehan, R. Storeng, D. Scudiero, A. Monks, J. McMahon, D. Vistica, J. T. Warren, H. Bokesch, S. Kenney and M. R. Boyd, *J. Natl. Cancer Inst.*, 1990, **82**, 1107–1112.
32. J. Panyam and V. Labhasetwar, *Adv. Drug Deliv. Rev.* 2003, **55**, 329–347.
33. E. Nogueira, A. Loureiro, P. Nogueira, J. Freitas, C.R. Almeida, J. Härmak, H. Hebert, A. Moreira, A.M. Carmo, A. Preto, A.C. Gomes and A. Cavaco-Pauloa, *Faraday Discuss.*, 2013, **166**, 417–429.
34. B. D. Chithrani, A. A. Ghazani and W. C. W. Chan, *Nano lett.*, 2006, **6**, 662–668.
35. K. Unfried, C. Albrecht, L. O. Klotz, A. V. Mikecz, S. G. Beck and R.P.F. Schins  
*Nanotoxicology*, 2007, **1**, 52–71.
36. N. Vij, T. Min, R. Marasigan, C.N. Belcher, S. Mazur, H. Ding, K.T. Yong and I. Roy, *J. Nanobiotechnology*, 2010, **8**, 22.
37. R. Gref, Y. Minamitake, M.T. Peracchia, V. Trubetskoy, V. Torchilin and R. Langer, *Science*, 1994, **263**, 1600–1603.

38. J. Park, P.M. Fong, J. Lu, K.S. Russell, C.J. Booth, W.M. Saltzman and T.M. Fahmy, *Nanomedicine*, 2009, **5**, 410–418.
39. T. M. LaVallee, X. H. Zhan, C. J. Herbstritt, E. C. Kough, S. J. Green and V. S. Pribluda, *Cancer Res.*, 2002, **62**, 3691–3697.
40. S. W. Fesik, *Nat. Rev. Cancer*, 2005, **5**, 995–995.
41. W.L. Scott and W.L. Athena, *Carcinogenesis*, 2000, **21**, 485–495.
42. J.L. Kipp and V.D. Ramirez, *Neuroendocrinology*, 2003, **77**, 258–272.



7x3mm (300 x 300 DPI)